Segmentation of white matter lesions from multimodal MRI in small vessel disease

Ana Isabel da Silva Loução Graça, *Biomedical Technology, Instituto Superior Técnico*

Abstract - **Cerebral Small Vessels Disease (SVD) is one of the main causes of cognitive impairment. Magnetic Resonance Image (MRI) has a high diagnostic and prognostic value for this kind of pathology. White matter lesions (WML) are one of the disease characteristic lesion types, which are most robustly detected as hyperintensities on images acquired using *Fluid Attenuation Inversion Recovery* (FLAIR) MRI. The WML load has high clinical relevance, and it is usually evaluated using qualitative scales by the neuroradiologist. However, a clear correlation cannot be found between WML load evaluated using these scales and disease progression. It would therefore been desirable to perform the segmentation of the WML's and subsequently quantify their volume. However, although several studies have addressed this issue, there is yet no standard, automatic method for WML segmentation.**

In this work, we propose an automatic WML segmentation methodology, which is based on the use of a common tissue segmentation algorithm available on a freeware software package for image processing – FSL – applied to multimodal MRI acquisitions, namely a FLAIR image and a T1-weighted image (T1-W). After pre-processing, the FAST algorithm was used for tissue segmentation into three tissue classes with a multi-channel approach taking both the FLAIR and T1-W images as input. Both images were co-registration to the standard MNI, and the white matter (WM) mask obtained by tissue segmentation of the MNI standard T1-W image was subtracted from the WM mask obtained by the individual tissue segmentation in each patient: the difference between these two WM masks should correspond to the WML's in each patient.

The proposed methodology was applied to images collected from a group of 16 patients with SVD. Sensitivity, specificity and accuracy were computed for each patient, through comparison with the ground truth obtained by manual segmentation of the WMLs. The Dice coefficient between the automatic and manual segmentation results was also computed. The average results belong to the best parameter set and were: sensitivity 40,73%; specificity 95,33%; Dice coefficient 0,23.

In summary, our proposed methodology, relying on standard and freeware tissue segmentation and co-registration tools, was able to achieve a WML segmentation with good sensitivity, specificity, and it may therefore yield a useful approach to WML quantification in SVD. Future work should investigate whether WML quantification obtained in this way may contribute a useful biomarker of SVD.

Key-words: Small Vessels Disease, White Matter Lesion, FLAIR, Segmentation, FSL

1. Introduction

Cerebral small vessels disease (SVD) is responsible for 20% of strokes worldwide, being the most common cause of dementia syndromes. [1], [2]. Different techniques can be used for SVD diagnostic and staging, however all SVD pathologies present white matter lesions (WML) hiperintensities in *Fluid Attenuation Inversion Recovery* (FLAIR) (magnetic resonance image (MRI) sequence). The WML is clinical relevant and neuroradiologists use semiquantitative scales such as the Fazekas scale to quantify the WML load (WMLL), which can be correlated with the clinical and neuropsychological evaluation of the patients. For this reason, the WML segmentation is fundamental for the diagnosis and monitoring of SVD pathologies.

This dissertation was developed in the scope of the research project *Neurophysim* (Noninvasive quantitative imaging of cerebral physiology: application to normal aging and small vessel diseases), led by the Institute for Systems and Robotics, Lisbon (ISR-Lisbon), in collaboration with Hospital da Luz. This project comprised the study of two patient populations: 1) sporadic SVD; and 2) Cerebral Autosomal Dominant Arteriopathy with Subcortical Infarcts and Leucoencephalopathy (CADASIL); this genetic pathology is considered a model of vascular dementia.

1.1. Small Vessels Diseases

SVD consist in a set of pathological processes that affect the small arteries, arterioles, capillaries and small veins [1]. Stroke is one of the main symptoms of cerebral SVD. Although the short-term prognostic of

this type of stroke are better when compared to other pathologies, the long-term prognostic is worse, being associated with high mortality and cognitive impairment. [3]. Other characteristics in cerebral SVD is the cerebral damage due to necrosis, to blood brain barrier disruption, to local inflammatory processes and to oligodendrocyte loss. SVD can be classified as sporadic or genetic. Almost of SVD is sporadic and is influence by a mix between genetic and cardiovascular risk [4]. SVD can be also organized based on its etiology: arteriolosclerosis, cerebral amyloid angiopathy, inherited/genetic SVD, inflammatory/immunologically mediated SVD, venous collagenosis and others (as post-radiation angiopathy) [1]–[3].

CADASIL is a hereditary disease of the small cerebral arteries and despite of not be the most prevalent SVD has characteristics that can clarify the physiological path of these pathologies. This disorder is caused by NOTCH3 mutations that are present in chromosome 19p13 [5], [6]. This gene encodes the trans-membrane receptor of 2321 aminoacids and it is only expressed by smooth muscles from the vascular wall [5]. Clinical presentations in CADASIL can change between and within families [7]. Some typical symptoms that CADASIL patients present are: migraine with aura, subcortical ischaemic events, mood disturbances, apathy and cognitive impairment. Ischaemic strokes are the most frequent manifestation in CADASIL, diagnosed in 60-85% of the patients [7]. Lacunar infarcts are responsible for some of the secondary symptoms, such as dysarthria, ataxia and non fluent aphasia [8].

1.2. Magnetic Resonance Image

In 1977 was acquired the first human MRI image [9] and since this discovery, MRI has revolutionized the diagnosis of innumerous clinical situations. Improvements in MRI hardware and software originated better image quality and reduced acquisition times [9], Also these improvements allows the acquisition of structural and functional information [10].

Magnetic resonance signal is produced after the release of energy that comes from the return of excited atomic nuclei to an equilibrium state [9]. Hydrogen (^{1}H) is the most abundant atom in the human body and it has only a proton in this nucleus. Moreover, its nucleus produces a strong MR signal. All these particularities, this charge and this spin nuclei turns ^{1}H into the most useful species for MRI. [11].

It is important to know some concepts to understand MRI:

- Spin-lattice relaxation: After excitatory pulses relaxation happens. It means that protons tend to return to their equilibrium state by transferring the energy to the environment – lattice. The time constant which defines the rate that excitatory protons return to equilibrium is namely spin-lattice or T1 relaxation time
- Spin-spin relaxation: The loss of transverse magnetization occurs though a process of spin-spin relaxation, with a time constant T2. It defines as the measure of the time taken for spinning protons to lose phase coherence among the nuclei spinning perpendicular field
- Repetition time: Repetition time (TR) is the time interval between multiple excitation pulses [11].
- Echo time (TE): It is defined as the time between the application of radiofrequency excitation pulse and the peak of the signal induced in the coil [11].
- T1-Weighted imaging (T1-W): In order to obtain T1 information, TR and TE should be shorted for T2 component suppression [15]. It is useful for visualizing the brain anatomy, because it provides excellent contrast between gray matter, white matter and CSF [14].
- T2-Weighted imaging (T2-W): It is based on the T2 time variations across tissues. [14]. T2-W images show changes in tissue intensity that are created by pathological factors [14]. To create T2-W images, the TR and TE should be long [15].
- Inversion recovery (IR): It occurs when there is the inversion of the initial magnetization in z axis. **T**he inversion time (TI) represents the delay between the inversion and excitation pulses. This procedure allows the elimination of normal tissues that can obscure pathological signal. Fluid-attenuated inversion recovery (FLAIR) is a T2-W sequence based on IR that is used for the suppression of CSF, increasing the contrast between lesions and normal brain tissues [13].

1.2.1. MRI in SVD

In neuroimaging, patients with SVD normally present lacunar and/or ischemic lesions like WML [2], [3]. Others characteristics of SVD in MRI are microbleeds, small subcortical infarcts, WM hyperintensities on FLAIR sequences, lacunes, prominent perivascular spaces and atrophy. Hyperintensities can also be visualized in subcortical grey matter (GM), such as in basal ganglia or inbrainstem [2]. Lacunar infarcts can be characterized on FLAIR sequence, presenting a central CSF-like hypointense and sometimes with a hyperintense border [2] and on T1-W by a hypointense signal [3]. Cerebral microbleeds have a hypointense signal in T2*-W. It is important to perform a careful analysis of this lesion type because it could be confused to some artifacts or other structures [2]. Other SVD's mark is superficial

cortical siderosis. This evidence can be observed in subarachnoid bleeding and it means that there are chronic blood products in the superficial cortex under piamater. T2*-W can identified it and it is characterized as hypointense signal [2].

T2-W and FLAIR sequences are two images modalities that present WML as hiperintensities. These lesions could be identify also in T1-W but with a isoitense or hypointense signal [2], [3]. FLAIR sequence also allows to differentiate the WML from lacunes or perivascular spaces [1], [2].

Diffusion tensor imaging (DTI), Magnetic Resonance Perfusion imaging with arterial spin labelling (ASL), and functional MRI (fMRI) have important results in SVD diagnosis, progression disease and pathophysiology research[1], [3]. Also other neuroimaging modalities can be used in the diagnosis of SVD, such as Single Photon Emission Computer Tomography (SPECT) and Positron Emission Tomography (PET). These modalities can have a role in some SVD especially by identifying metabolic defects such as hypometabolism (^{18}F-FDG PET image), by establishing amyloid burden (^{11}C-PiB PET image) and by analyzing cerebral perfusion (^{99m}Tc-HMPAO SPECT image) [1].

1.3. Lesion segmentation

Segmentation is the classification of pixel from an image into different groups with the same features such as intensity or texture [12]. This method can be apply to MRI brain imaging and is a very important issue for some clinical practice situations such as surgical planning, multimodality image registration, lesions quantification, separating into different cerebral regions (CSF, WM,GM), etc [12], [13]. All over the years experts try to choose the best segmentation methodology for these applications without success.

Segmentation methodology can be classified based on human intervention: manual segmentation, semi-automatic segmentation and automatic segmentation [14]. In manual segmentation method the image is labelled slice-by-slice and segmented by hand which can be influenced by artifacts and image quality. It is used nowadays in the evaluation of automatic segmentation through the "ground truth" definition [15]. Ideally semi-automatic or automatic methods should be preferred [12].

Some research has been made to solve this problem and several algorithms were created and improved such as: intensity-based, thresholding, region growing, edge detection, classifiers, clustering, statistical models, artificial neural networks (ANN), deformable models and atlas-guided approaches. Some authors, in the attempt to obtain more accurate segmentation results, conjugate different methods [12].

Expectation maximization (EM) and Markov Random Field model (MRF) are two examples of statistical models. The combination of these to algorithms are the basis of the FSL segmentation tool – FAST [15].

1.3.1. Lesion segmentation in SVD

In the last years lesions segmentation in MRI had been a challenge that a lot of researchers try, without success, to solve. Here will be presented some of the research works that address the lesions MRI segmentation issue. Some of the papers are not focus only in SVD, however pathologic lesions presented are similar and some strategy of these methods could be important to apply in SVD in future.

Karthik et al (2016) apply wavelet functions in segmentation image for discriminated lesions from normal brain tissue and concluded that its presents higher differentiation in the discrimination healthy tissue from pathologic tissue[16].

K-NN was used by Anbeek et al (2004). The authors used a multiple spectral approach (T1-W, IR, Proton Density (PD), T2-W, FLAIR) and concluded that this technique has a high sensitivity and specificity by ROC curves. [17].

Si and Bhattacharjee (2016) develop an algorithm for detect MRI brain lesions without tissues classification. For solve this problem the authors created a classifier that uses a Multi-Layer Perceptron neural network, which is trained by Levenberg-Marquardt method. The method present a good results in specificity, accuracy and dice coefficient. However authors think that better results could be obtained associated this method to wavelet features [18].

Lesion Identification with Neighborhood Data Analysis (LINDA) was proposed by Pustina et al (2016). It is a supervised algorithm segmentation that uses information from each voxel and their neighborhood and promoted hierarchical improvements of lesion estimation [19]. The authors only applied one image modality (T1-W) for analyzed chronic stroke lesions and they employed a Random Forests approach that leads a good accuracy results. This algorithm presents a high sensitive results and can generated a graded posterior probability maps that exhibit the model uncertainty [19].

FMRIB's Automated Segmentation Tool (FAST) uses a hidden Markov Random Field model (HMRF) propose by Zhang et al (2001). The authors used MRF that do not observe directly the generation of stochastic process that it produces but can determinate the process from the field observations. Also to estimate model

parameters it was applied EM algorithm. The two approaches together improve the accuracy and robustness of the algorithm segmentation [20].

1.4. Goals

WML segmentation in SVD can be time-consuming and can produce inaccurate results. In the last years more accurate results are searched by using automatic or semi-automatic techniques; however it is an unsolved problem because there is no optimal method for all pathologies. Nowadays, there is no recommended method for this issue and new algorithms still be proposed. On the other hand, there are free tools that can be used for image segmentation, but there are no specific guidelines for their utilization in WML and SVD.

The main aim of this study is to create a WML segmentation pipeline, to be applied to SVD, based on pre-existing and freely available segmentation algorithms. To accomplish this main object, the following specific objectives were defined:

- Skull stripping optimization
- Achieve optimal results for inter and intra subjects registration
- Achieve optimal results in tissue segmentation
- Produce an accurate gold standard

2. Materials and Methods

2.1. Study Population

From January 2015 to January 2016, brain MRI images were acquired at Hospital da Luz, Lisboa, in the scope of the Neurophysim project, following appropriate inclusion criteria and upon informed consent from all participants, according to the approval by the local Ethical Committee.

The study population analyzed in this thesis is composed by16 subjects (5 men and 11 women) with a mean age of 52 ± 11 years old. All the subjects have a diagnosis of SVD, four of them with the subtype CADASIL.

2.2. Acquisition Protocol

The imaging data was acquired in a 3T Siemens Verio MRI system, following a comprehensive protocol. The images analyzed were a T1-W image obtained using an MPRAGE sequence and a FLAIR image. Acquisition parameters for MPRAGE were: image size of 144x240x254 pixel with a sagittal acquisition orientation, a slice number of 160, a slice thickness with 1mm and no spacing between slices. TR, TE and TI are respectively 2250ms, 2,26ms and 900ms. For FLAIR acquisition the parameters were: image size of 256x320x45 pixel with a transaxial acquisition orientation, a slice number of 47, a slice thickness with 3mm and a spacing between slices of 3,3mm. TR, TE and TI are respectively 8500ms, 97ms and 2500ms.

2.3. Image Processing

The following processing steps were performed for lesion segmentation, including: pre-processing by skull stripping and brain extraction; co-registration of MPRAGE and FLAIR images, and normalization to MNI space; tissue segmentation in three classes (WM, GM and CSF); and finally WML segmentation. The FSL (FMRIB Software Library v5.0) software package was used for all the steps of image processing.

It was used for skull stripping and brain extraction we used the Brain Extraction Tool (BET) from FSL software [21]. In some images BET did not yield good results in skull striping, so we performed manual brain extraction.

2.3.1. Image registration

For our proposed segmentation process requires not only the intra-subject image co-registration (T1-W and FLAIR), but also image normalization with a standard image from the Montreal Neurologic Institute (MNI-152).

All registration operations were performed using FMRIB's Linear Image Registration Tool (FLIRT). Firstly we register FLAIR in T1-W space by linear transformation using FLIRT and the parameters were: cost function *corratio;* interpolation trilinear function; angles chosen for the first optimization step are -90º and +90º for both x and z directions; both 6 and 12 degrees of freedom (DOF) were tested.

For the registration of the T1-W image with the MNI image, we first employed a linear registration step using FLIRT, with 12 DOF, and otherwise identical options to the previous registration. Subsequently, a non-linear registration step is also employed using FMRIB's nonlinear image registration tool (FNIRT) [22] and a warp is obtained from the FNIRT process for T1-W creation in MNI space. FNIRT parameters were defined in file configuration recommended (T1_2_MNI152_2mm). We also tested running FNIRT using a one more *lambda* value (lambda=8), in the attempt to improve registration.

The non-linear warp is inverted and concatenated, to register any image in the MNI standard space into the FLAIR space of each subject.

The segmentation of the MNI template brain image is performed using default options, into GM, WM and CSF. Because this image corresponds to the standard, template brain, it does not present any WMLs.

2.3.2. Lesion Segmentation

To obtain a segmentation of the WMLs, we subtract the WM mask obtained by multichannel segmentation of T1-W and FLAIR into three classes from the WM mask obtained from the MNI standard image. In order to eliminate residual errors of this subtraction in superficial cortical regions, we apply the BET tool to the WML mask, using an appropriate fractional intensity threshold of 0,8, 0,9 or 1.

2.3.3. Tissue segmentation

Tissue segmentation is performed, based on the patient's individual images as well as on the MNI template brain image, using FLS's tool FAST[41].

For the segmentation of the patient's individual images we tested two methodologies: a multichannel, modality (using both T1-W and FLAIR images) and a one-channel modality using either T1-W or FLAIR images. It each case, we also tested three or four classification classes.

Initially, we attempted to achieve the automatic separation of WMLs from the three normal tissues, GM, WM and CSF, by using four classes instead of three, and providing both the FLAIR as well as the MPRAGE images as input to the multispectral segmentation algorithm. However, this approach was not successful. In fact, WMLs were systematically classified as GM or CSF, even when four classes were segmented. Alternatively, we attempted a different approach to obtain a WML segmentation, which involved the comparison of the patient's WM mask with that of a template brain, without WMLs.

The segmentation of the MNI template brain image is performed using default options, into GM, WM and CSF. Because this image corresponds to the standard, template brain, it does not present any WMLs.

2.3.4.Performance Evaluation

Qualitative and quantitative analysis was performed. For qualitative measures we observe all the segmented images and for quantitative evaluation true positive (TP), false positive (FP), true negative (TN) and false negative (FN) are calculated. Also we used the following outcome measures, by comparison with a ground truth, obtained by manual segmentation of WMLs (using the same intensity range in all the cases, 0-1100):

The Dice coefficient (DC) is calculated by [23], [24]:

$$\mathrm{DC} = \frac{2 \times (\mathrm{GT} \cap \mathrm{Seg})}{\mathrm{GS} + \mathrm{Seg}}$$

where GT is a ground truth segmentation and Seg is an automated segmentation.

The sensitivity, specificity and accuracy are calculated by [25] [26]:

$$\text{Sensitivity} = \frac{\mathrm{TP}}{\mathrm{TP} + \mathrm{FN}}$$

$$\text{Specificity} = \frac{\mathrm{TN}}{\mathrm{TN} + \mathrm{FP}}$$

$$\text{Accuracy} = \frac{\mathrm{TP} + \mathrm{TN}}{\mathrm{TP} + \mathrm{FP}}$$

The percentage and of lesion volume non detected (LVND) is calculated by:

$$\%\ \text{Lesion volume non detect} = \frac{\mathrm{GT} - \mathrm{TP}}{\mathrm{GT}} \times 100$$

$$\mathrm{LVND} = \frac{\mathrm{GT\ volume}\ \times\ \%\ \text{Lesion volume non detected}}{100}\ (cm^3)$$

3. Results

The methodology implemented has the objective to achieve the optimal result in each step. Bad results in one step can promote lesion segmentation without quality.

Skull stripping was applied to all brain MRI images. More accurate results were obtained changing the center of gravity of the initial mesh surface in each image which should be located between and slightly above ventricles. Manual segmentation was required in 6 T1-W and in 3 FLAIR images.

Intra-subject registration results with different DOF in FLIRT do not change significantly. However inter-subject registration results differ between using FLIRT or FNIRT, i.e., with FLIRT it is observed problems in tissue correlation close to ventricles. Despite better registration results, FNIRT registration bring us another problem. Both FNIRT registrations classify lesions areas as GM instead of classifying as WM. Also,

adding a lambda=8 in FNIRT registration led to some improvements (Figure 1).

Different tissue segmentation was proposed. When we employed a multi-channel strategy (T1-W and FLAIR) the results seems to be more accurate. In three classes, we are able to separate WM in all cases. WML are also classified as GM in all cases and sometimes as CSF. However, when we employed a four classes classification the results do not improve.

Lesion segmentation is based on multi-channel approach with three classes and is the result of the subtraction of the WM from MNI and the WM from multi-channel data (FLAIR and T1-W). Qualitatively, in most cases, lesions close to ventricles are not classified as lesions. Moreover some GM tissue was classified as lesion. These are two sources of lesions identification error that were found.

The subjects with a low WML load had more GM classified as lesion than true lesions. When we apply BET with a fractional intensity threshold some of the GM tissue disappear. This phenomenon is bigger with a high threshold value, however with high threshold some lesions are nullified (Figure 2)

The quantitative results support the qualitative evaluation. Higher sensitivity values were founded when we do not apply BET (FNIRT standard with a mean of 48,89 % ±11,49 % and FNIRT lambda=8 with a mean of 40,73 % ± 12,52 %). The sensitivity value tend to decrease with higher BET fractional intensity threshold (Figure 5).

Specificity and accuracy results have the inverse behavior when comparing with sensitivity. So, FNIRT with BET and high a fractional intensity threshold present better results. Also the results are generally

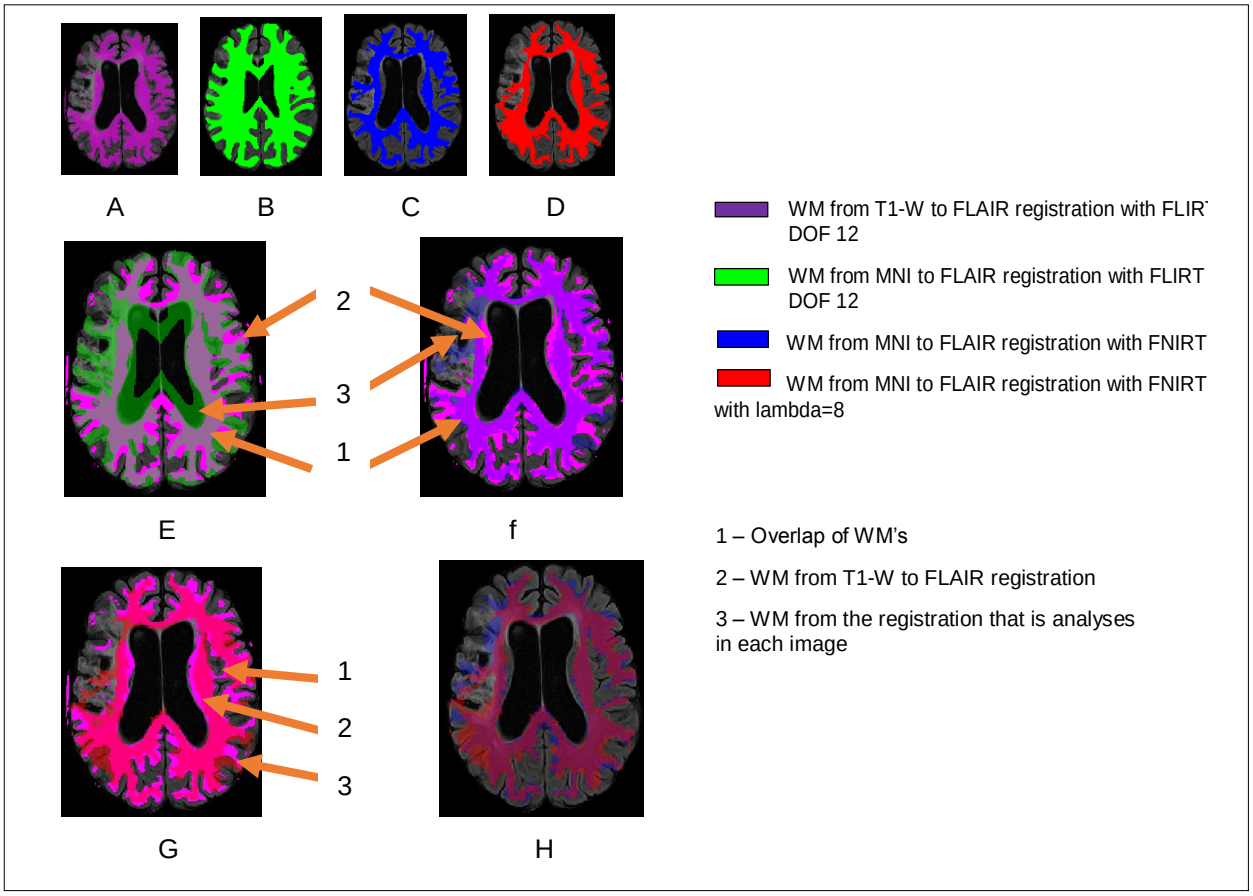

***Figure 1**: Registration results. Comparison between the WM from different registrations. A - WM from T1-W to FLAIR registration with FLIRT DOF12; D - WM from MNI to FLAIR registration with FLIRT DOF 12; C - WM from MNI to FLAIR registration with FNIRT; D - WM from MNI to FLAIR registration with FNIRT with lambda=8; E – Comparison between WM T1-W to FLAIR registration and WM MNI to FLAIR registration with FLIRT DOF 12; F – Comparison between WM T1-W to FLAIR registration and WM MNI to FLAIR registration with FNIRT; G – Comparison between WM T1-W to FLAIR registration and WM MNI to FLAIR registration with FNIRT lambda=8; H - Comparison between WM MNI to FLAIR registration to FNIRT and WM MNI to FLAIR registration with FNIRT lambda=8.*

higher with FNIRT lambda=8 as observed in Figure 5. For specificity and accuracy the higher value belongs to FNIRT lambda=8 (98,92% ± 0,26% and 97,08 %±1,71% respectively).

behavior of this evaluated parameter is similar to sensitivity. So, with higher a BET fractional intensity threshold parameter, higher is the lesion volume that it is not identified.

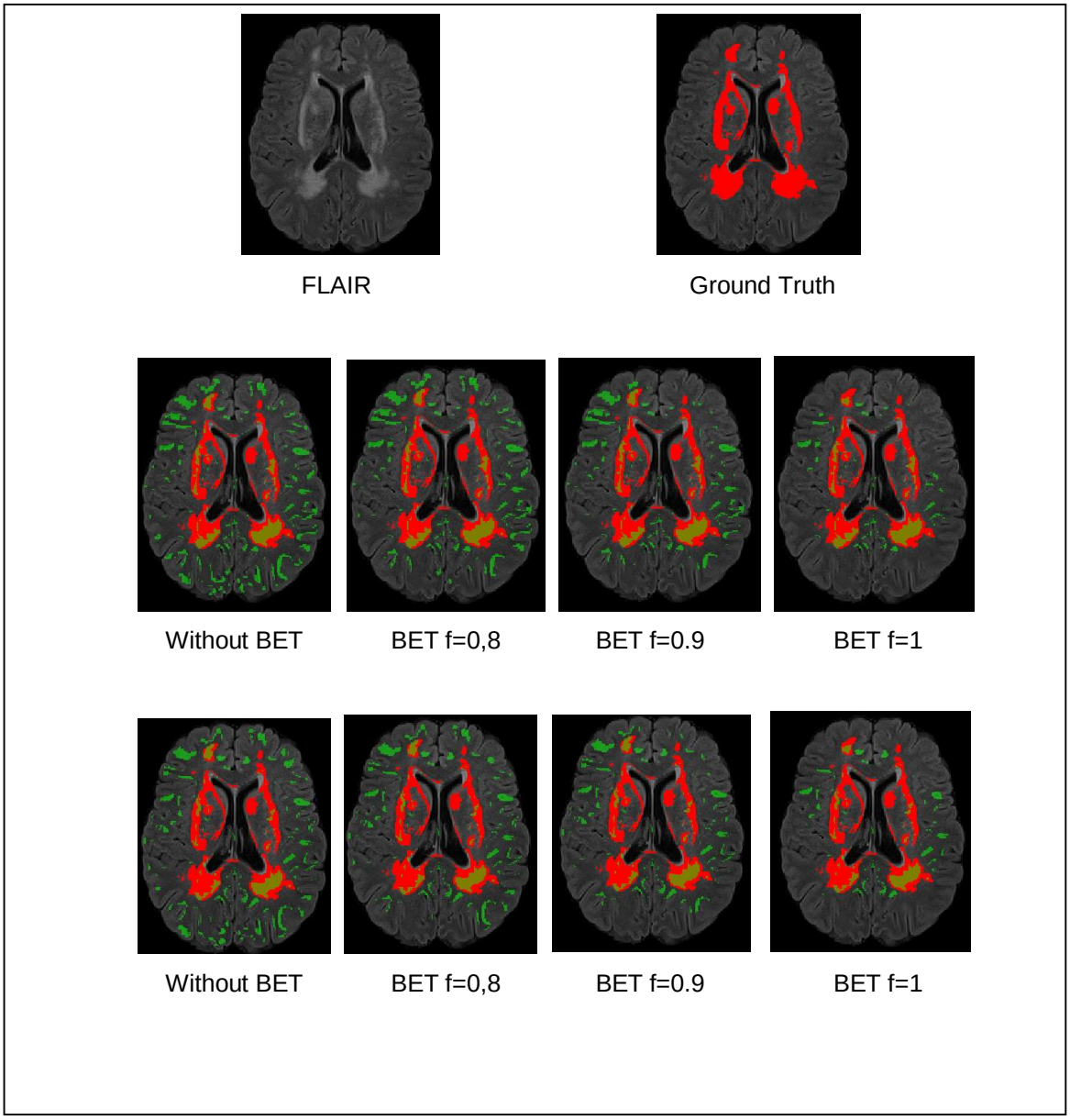

Figure 2: *WML segmentation results obtained by different methods*

DC results follow the same trend of specificity and accuracy results. Also it is observed a high difference between the two FNIRT registrations without BET. FNIRT with lambda=8 has a DC value double than FNIRT standard (0,23±0,12 and 0,13±0,08 respectively). However we are able to increase this value with the BET application, higher the fractional intensity threshold, higher is DC (Figure 3).

We also analyzed the lesion identification error. The

However all the values are high, with BET fractional intensity threshold parameter of 1, the percentage of not identified lesions are higher than 70%. The results can be observed in Figure 4.

In Figure 5 all the parameters are compared to understand which is the best option. After graphical analyses FNIRT standard is more susceptible to BET influence than FNIRT lambda=8. Also, FNIRT lambda=8 without BET application seems to have good

results because do not have low accuracy and specificity and presents an intermediate DC result. Sensitivity result is not reasonable comparing to others results and the volume of lesion that is not identified by automatic segmentation is not the worst.

4. Discussion

This study aimed to develop a pipeline for automatic WML segmentation of MRI images from SVD patients.

Skull stripping is required for image registration and segmentation, however automatic method do not achieve good results in 9 MRI images which need a manual skull stripping, that is time consuming. Popescu et al in the attempt to optimize parameters to increase BET performance in T1-W images concluded that for some acquisitions protocols the results are not satisfactory and the reason is the amount of neck slices present [27].

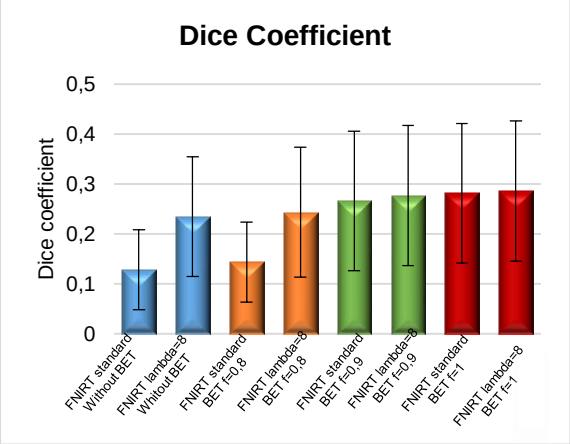

Figure 3: *Group average DC results (error bars represent SD).*

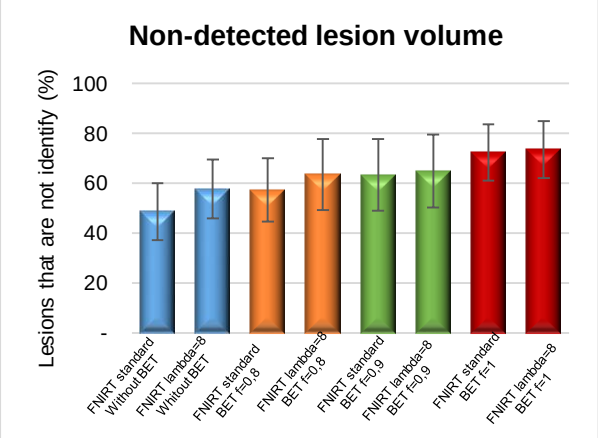

Figure 4: *Group average non detected lesion volume results (error bars represent SD).*

Also, Leung et al. compared four methods of brain extraction and concluded that this protocol tend to exclude temporal and frontal lobe as well as cerebellum. In our study, bad BET results present the same lake in frontal lobe and cerebellum tissue.

In our work, registration has the objective to transport T1-W to the FLAIR space to a multichannel segmentation with FAST. Also registration with MNI is required. We employed FLIRT for T1-W and FLAIR registration between same individuals and the results are

accurate. However when we register MNI whit T1-W and FLAIR is not so positive because there are brain structural differences between a standard and a real patient brain. FNIRT registration demonstrates more accurate results than FLIRT for these cases and seems to more perfect with the application of lambda=8. However, better results are required to increase the segmentation performance.

Other request for this study is that all the images

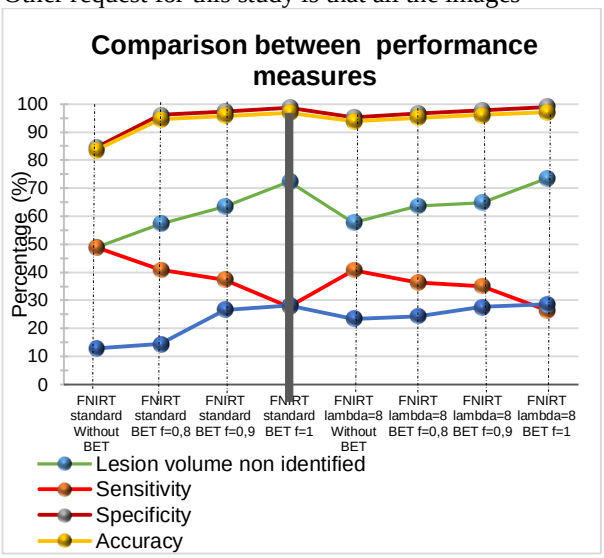

Figure 5: *Comparison between the different performance measures for the different pipeline options tested. Grey line divided the results obtained by using different BET in FNIRT standard and in FNIRT lambda=8.*

should be in FLAIR space. The reason is related with the fact that one of the MRI images characteristics for SVD is hyperintensities in WM on FLAIR sequence. If the study was not drawn in this space, lesions alteration could be appearing and the results will suffer a bias. So it is important to work with the data in the original space for more accurate results.

Other step analyzed was tissue segmentation. Three classification classes have better results when compared with four classes. The main idea to use a four classes approach comes from the possibility that, with a multi-channel registration, lesions appear as a fourth class. WML hyperintensities in FLAIR can be visualized as hypointense signal in T1-W brain image.

FAST uses a MRF model. This model is characterized by mutual influences between pixel [12]. If we conjugate the images, maybe the model could identify the hyperintensities in FLAIR in same locations of hypointensities in T1-W and identifies as another class.

In this case, integrating both images reduce the uncertainty and increase the accuracy of segmentation. Admiraal-Behoul et al also uses a multi-channel approach (PD, T2-W and FLAIR) for the same fact [18].

Tissue segmentation was required not only to separate WML but also to separate WM from other classes. So, if we are not able to put WML in a single class we need to change the approach. Thus, in patient's WM we know that pixel where lesions are located do not belong to WM class and if we subtract this WM with the WM of a pattern without lesions (MNI's WM) we should obtain the WML images. However, in our research, this is not true. One possibility for this outcome is a not perfect registration. Almost all the lesions which have an incorrect classification are close to the ventricles and outside brain regions (GM are incorrectly classified as a lesion). The reason for this result is a non-optimal registration that leads to errors classifications in MNI and this missclassified tissue in MNI becomes FN or FP. Besides that with big lesions FAST classifies MNI images as GM, so when we applied the subtraction there is no WM in MNI image in the lesion location. This problem is more obvious when we use a better registration (FNIRT with lambda=8) and can be a reason for less sensitivity
in this case.

To brush away some misclassified pixels, we used the fractional intensity threshold from BET parameters. This automatic segmentation, with a higher fractional intensity threshold, has high specificity values, however the sensitivity values are not so satisfactory. The accuracy results are reasonable. Discrepancies of the sensitivity results between patients are high in all cases [25].

The reason for specificity measures (higher values with higher fractional intensity threshold) is the elimination of GM tissue that was misclassified [25].

The accuracy of FNIRT with lambda=8 and fractional intensity threshold of 1, is 97,08% , the higher value obtained.

DC reasonable value is higher than 0,7 [21], [28]. Our results are very low comparing with this value (all of the DC mean values are less than 0,3) and better DC results come from patients with a high WML load.

An important result is the lesion quantification that is not identified by the automatic segmentation. The values are high and trend to increase when we apply BET. However it is not satisfactory for clinical practice yet.

FNIRT lambda=8 without BET application seems to be the more consensual when we analyze all the results. It does not have the best result in any evaluated parameter but when we proceed to the comparison between all of the methods used it is the methodology that have more true results and it is capable to identified a high lesion percentage. When comparing the results with other studies the results are not satisfactory. Anbeek et al [24], Si et al [18], Admiraal-Behloulet al [28], Jokinen et al[29] Pustina et al [19], Strumia et al [30] concluded that a small WML load have worse results than with the high lesion load. So this is in agreement with our results. However the algorithm that these authors proposed have higher DC results than ours. Table 1 shows the different DC results from papers.

Table 1: *Different DC results from papers*

Papers	DC
Anbeek et al	0,81
Si et al	0,87
Admiraal-Behloul et al	0,75
Pustina et al	0,70
Strumia et al	0,520

A study limitation is the gold standard that should be done by an expert however this was not possible. This detail turns this work less accurate because experience in MRI brain visualization is fundamental to achieve better results in ground truth. Other disadvantage of this pipeline is also time consuming for some steps.

Using a free framework is the biggest advantage, because all people can use it. There are other free frameworks for lesions segmentation and quantification. MSMetrix is available in https://msmetrix.icometrix.com. The big disadvantage of MSMetrix is that we only have access to the report of lesion segmentation and we are not able to visualize all the slices. So is a blind user framework that requires all users to believe in the result that give us.

5. Conclusion

Characterization of WM hyperintensites on FLAIR images is an important feature for diagnosis and prognosis of SVD and this could be possible through WML segmentation.

The images processing is done in a slow framework. Also the results are not so positive. Towards these results, changes in the methodology should be done.

For future work, we could apply vertical gradient in fractional intensity. This can cut off more FP pixels and

reserve the TP pixels eliminated in this procedure. Other possibility is the registration of PD images with FLAIR and T1-W that can improve tissue segmentation because of FLAIR hyperintensities artifacts. The application of this registration will produce more accurate tissue segmentation and maybe more accurate lesion segmentation. Also, it could be important to investigate if WML quantification obtained in this way may contribute a useful biomarker of SVD

One of the problems report is the inter-subject registration. More accurate registration outcomes promote a better WML classification. Results from FNIRT are satisfactory but if we change some parameters such as lambda we believe that a better WM registration is possible from the MNI and FLAIR images. Also, a more correct WML classification is achieved.

Other possible strategy is using the GM tissue mask instead of WM, because the majority of hyperintense WML belongs to GM classification and the other lesions that are not as GM are lacunes and belongs to CSF

We think that better results are possible with this free framework. However more parameters should be analyzed in future works and maybe a more efficient pipeline will be obtained.

Acknowledgements

I acknowledge the NeuroPhysIm Project, and its participating institutions and researchers, in the scope of which this thesis was conducted.

References

[1] G. Banerjee, D. Wilson, H. R. Jäger, and D. J. Werring, "Novel imaging techniques in cerebral small vessel diseases and vascular cognitive impairment," *Biochim. Biophys. Acta - Mol. Basis Dis.*, vol. 1862, no. 5, pp. 926–938, 2016.

[2] J. M. Wardlaw, E. E. Smith, G. J. Biessels, et al, "Neuroimaging standards for research into small vessel disease and its contribution to ageing and neurodegeneration," *Lancet Neurol.*, vol. 12, no. 8, pp. 822–838, 2013.

[3] L. Pantoni, "Cerebral small vessel disease : from pathogenesis and clinical characteristics to therapeutic challenges," *Lancet Neurol.*, vol. 9, no. 7, pp. 689–701, 2010.

[4] A. Joutel and F. M. Faraci, "Cerebral Small Vessel Disease," *Stroke*, vol. 45, no. 4, pp. 1215–1221, 2014.

[5] R. N. Kalaria, M. Viitanen, H. Kalimo, et al, "The pathogenesis of CADASIL: An update," *J. Neurol. Sci.*, vol. 226, no. 1–2 SPEC.ISS., pp. 35–39, 2004.

[6] M. Dichgans, M. Mayer, I. Uttner, et al, "The Phenotypic Spectrum of CADASIL : Clinical Findings in 102 Cases," *Ann Neurol*, vol. 44, no. 5, pp. 731–739, 1998.

[7] H. Chabriat, A. Joutel, M. Dichgans, E. Tournier-Lasserve, and M. G. Bousser, "Cadasil," *Lancet Neurol.*, vol. 8, no. 7, pp. 643–653, 2009.

[8] H. Chabriat and M. Bousser, "CADASIL (' cerebral autosomal dominant arteriopathy with subcortical infarcts and leukoencephalopathy ') Cerebral autosomal dominant arteriopathy with subcortical infarcts and leukoencephalopathy (CADASIL)," *EMC-Neurologie*, vol. 1, no. 2, pp. 156–168, 2004.

[9] T. Ai, J. N. Morelli, X. Hu, et al, "A historical overview of Magnetic Resonance Imaging, focusing on technological innovations.," *Invest. Radiol.*, vol. 47, no. 12, pp. 725–741, 2012.

[10] M. F. Reiser, W. Semmler, and H. Hricak, *Magnetic Resonance Tomography*. Springer Science & Business Media, 2007.

[11] H. S. Chrysikopoulos, *Clinical MR Imaging and Physics*, Springer. Corfu, 2009.

[12] R. Xu, L. Luo, and J. Ohya, "Segmentation of Brain MRI," in *Advances in brain Imaging*, V. Chaudhary, Ed. Shangai: In Tech, 2012, pp. 143–170.

[13] J. A. Shah and S. R. Suralkar, "A Review on Brain Tumor Segmentation Techniques for MRI Images," in *International Conference on Global Trends in Engineering, Technology and Management (ICGTETM-2016)*, 2016, pp. 323–330.

[14] N. M. Zaitoun and M. J. Aqel, "Survey on Image Segmentation Techniques," *Procedia - Procedia Comput. Sci.*, vol. 65, no. Iccmit, pp. 797–806, 2015.

[15] I. D. T, B. Goossens, and W. Philips, "MRI Segmentation of the Human Brain : Challenges , Methods , and Applications," *Comput. Math. Methods Med.*, vol. 2015, pp. 1–23, 2015.

[16] R. Karthik and R. Menaka, "Statistical characterization of ischemic stroke lesions from MRI using discrete wavelet transformation," *ECTI Trans. Eletr. Eng. Electron. Commun.*, vol. 14, no. 2, pp. 57–64, 2016.

[17] P. Anbeek, K. L. Vincken, M. J. P. Van Osch, et al, "Probabilistic segmentation of white matter lesions in MR imaging," *NeuroImag*, vol. 21, no. 3, pp. 1037–1044, 2004.

[18] T. Si, A. De, and A. K. Bhattacharjee, "Artificial Neural Network based Lesion Segmentation of Brain MRI," *Commun. Appl. Electron.*, vol. 4, no. 5, pp. 1–5, 2016.

[19] D. Pustina, H. B. Coslett, P. E. Turkeltaub, et al, "Automated Segmentation of Chronic Stroke Lesions Using LINDA : Lesion Identification With Neighborhood Data Analysis," *Hum. Brain Mapp.*, vol. 1421, no. 4, pp. 1405–1421, 2016.

[20] Y. Zhang, S. Smith, and M. Brady, "Hidden Markov Random Field Model and Segmentation of Brain MR Images," *IEEE Trans. Med. Imaging*, vol. 20, no. 1, pp. 45–57, 2001.

[21] P. Anbeek, K. L. Vincken, G. S. Van Bochove, M. J. P. Van Osch, et al, "Probabilistic segmentation of brain tissue in MR imaging," *Neuroimage*, vol. 27, no. 4, pp. 795–804, 2005.

[22] J. L. R. Andersson, M. Jenkinson, and S. M. Smith, "Non-linear optimisation. FMRIB technical report TR07JA1," 2007.

[23] L. R. Dice, "Measures of the Amount of Ecologic Association Between Species," *Ecology*, vol. 26, no. 3, pp. 297–302, 1945.

[24] P. Anbeek, K. L. Vincken, M. J. P. Van Osch, et al, "Automatic segmentation of different-sized white matter lesions by voxel probability estimation," *Med. Image Anal.*, vol. 8, no. 3, pp. 205–215, 2004.

[25] A. G. Lalkhen and A. McCluskey, "Clinical tests: Sensitivity and specificity," *Contin. Educ. Anaesthesia, Crit. Care Pain*, vol. 8, no. 6, pp. 221–223, 2008.

[26] R. H. Riffenburgh, *Statistics in Medicine*, vol. 1. Acaademic Press, 2012.

[27] V. Popescu, M. Battaglini, W. S. Hoogstrate,et al, "Optimizing parameter choice for FSL-Brain Extraction Tool (BET) on 3D T1 images in multiple sclerosis," *Neuroimage*, vol. 61, no. 4, pp. 1484–1494, 2012.

[28] F. Admiraal-Behloul, D. M. J. Van Den Heuvel, H. O. M. J. P. Van Osch, et al, "Fully automatic segmentation of white matter hyperintensities in MR images of the elderly," *NeuroIma*, vol. 28, no. 3, pp. 607–617, 2005.

[29] H. Jokinen, N. Gonçalves, R. Vigário, et al, "Early-Stage White Matter Lesions Detected by Multispectral MRI Segmentation Predict Progressive Cognitive Decline," *Front. Neurosci.*, vol. 9, no. December, pp. 1–9, 2015.

[30] M. Strumia, F. R. Schmidt, C. Anastasopoulos, et al, "White Matter MS-Lesion Segmentation Using a Geometric Brain Model," *IEEE Trans. Med. Imaging*, vol. 34, no. 7, pp. 1636–1646, 2016.